IEEE Photonics Journal
An IEEE Photonics Society Publication

Open Access

Terahertz Absorber With Reconfigurable Bandwidth Based on Isotropic Vanadium Dioxide Metasurfaces

Volume 11, Number 2, April 2019

Zhengyong Song
Maoliang Wei
Zhisheng Wang
Guoxiong Cai
Yineng Liu
Yuanguo Zhou

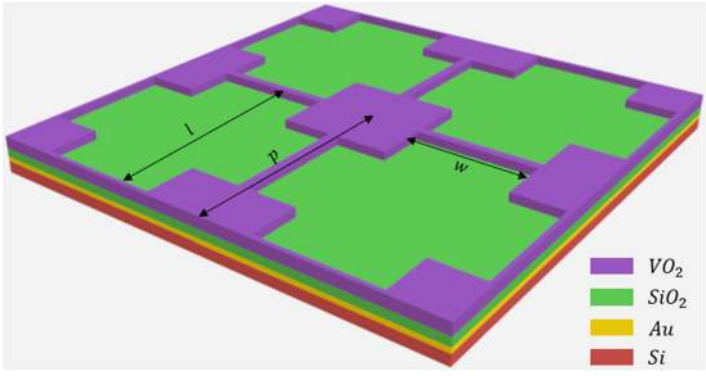

DOI: 10.1109/JPHOT.2019.2898981
1943-0655

IEEE photonics SOCIETY

IEEE

Terahertz Absorber With Reconfigurable Bandwidth Based on Isotropic Vanadium Dioxide Metasurfaces

Zhengyong Song,[1] **Maoliang Wei**,[1] **Zhisheng Wang**,[1] **Guoxiong Cai**,[1] **Yineng Liu**,[1] **and Yuanguo Zhou**[2]

[1]Department of Electronic Science, Institute of Electromagnetics and Acoustics, Xiamen University, Xiamen 361005, China
[2]College of Communication and Information Engineering, Xi'an University of Science and Technology, Xi'an 710054, China

DOI:10.1109/JPHOT.2019.2898981

Manuscript received January 7, 2019; revised February 2, 2019; accepted February 7, 2019. Date of current version February 26, 2019. This work was supported by the National Natural Science Foundation of China under Grant 11504305. Corresponding authors: Zhengyong Song and Yuanguo Zhou (e-mail: zhysong@xmu.edu.cn; wingkoo@foxmail.com).

Abstract: The design of a broadband tunable absorber is proposed based on a thin vanadium dioxide metasurface, which is composed of a simple array of vanadium dioxide and a bottom gold film. When the conductivity of vanadium dioxide is equal to 2000 Ω^{-1}cm^{-1}, simulated absorptance exceeds 90% with 71% bandwidth from 0.47 to 0.99 THz and full width at half maximum is 98% from 0.354 to 1.036 THz with center frequency of 0.695 THz. Simulated results show that absorptance peak can be tuned from 5% to 100% when the conductivity changes continually from 10 Ω^{-1}cm^{-1} to 2000 Ω^{-1}cm^{-1}. The designed absorber may have useful applications in terahertz spectrum such as energy harvesting, thermal emitter, and sensing.

Index Terms: Absorber, metasurface, vanadium oxide.

1. Introduction

In the past several years, metamaterial absorber (MMA), one kind of electromagnetic absorber made of metamaterial (MM) resonators, has been attracting great attention and making huge progress [1]–[17]. Most of the proposed MMAs are composed of two metallic layers separated by dielectric material. Subwavelength micro- and nano-structures based on metal-insulator-metal (MIM) are often employed to get perfect absorption, and localized surface plasmon polaritons (LSPPs) exhibit an absorption independent on incident angle. Such absorbers are very promising for various applications, such as photodetector [2], [3], photovoltaic cell [4], [5], and stealth technology [6], [7]. However, absorption bandwidths of these MMAs are frequently narrow since LSPP resonance is limited in most cases to a single resonant mode. Absorption spectra can be widened by combining different structures with different widths, sizes, and shapes. In order to improve bandwidth, some efforts have been made from microwave [8], [9], terahertz [10], [11] to optical frequencies [12], [13], which often includes multiple resonators with different sizes [14], [15] or multilayer structure with different geometrical dimensions [16], [17]. T. Jang *et al.* designed an optically transparent, flexible, and polarization-insensitive broadband microwave absorber [9]. It is designed to have two

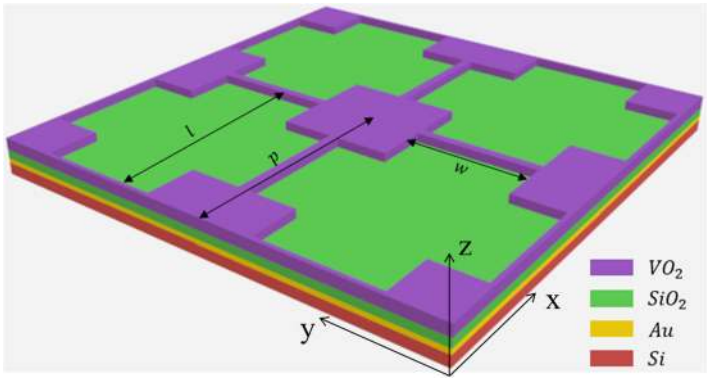

Fig. 1. Schematic of the designed broadband absorber, consisting of periodic air cross hole in VO_2 film (purple), a silica spacer (green), and the gold film (yellow). The whole system is deposited on silicon (red) substrate.

overlapping resonances of the bow-tie array, which originates from the fundamental resonance mode and the coupling between the adjacent elements. Z. Song *et al.* studied a wideband absorber based on a silicon terahertz metasurface [11]. L. Lei *et al.* presented a design of an ultra-wideband absorber consisting of titanium-silica periodic cubes and an aluminum substrate [13]. H. Deng *et al.* demonstrated a broadband absorber with infrared wavelength ranging from 1 μm to 5 μm. It has two stacked chromium ring resonators on a reflective chromium mirror [17]. The configurations of these designs are not simple, and they require some complicated fabrication procedures. At the same time, the position and intensity of absorption peak are usually unchanged once the structure of MMA is fabricated [18]–[25].

In potential applications, tunable absorber is more attractive for the smart design. So dynamically tunable absorbers with the simple structure are desired. The transition behavior of vanadium oxide (VO_2) between insulator and metal is well known around 340 K. With the increase of temperature, lattice structure of VO_2 changes from monoclinic to tetragonal structure, and the corresponding electrical conductivity increases by several orders of magnitude during transformation process. It has wide potential in temperature sensitive photonic, electronic, and thermal devices. Combining MM with VO_2 thin film or small particle is a promising way to dynamically regulate electromagnetic properties of some practical devices [26]–[31]. In 2010, W. Huang *et al.* presented a *gold strip*/VO_2 *spacer*/*gold strip* sandwich MM to study the optical response [26]. Their results show that nanostructures can be used as dynamic temperature-controlled optical switch. In 2012, M. A. Kats *et al.* showed perfect absorption in a single lossy VO_2 layer [27]. The design generates 99.75% absorption at $\lambda = 11.6$ μm. In 2015, H. Kocer *et al.* demonstrated a thermally tunable short-wavelength infrared resonant absorber by heating up hybrid gold-VO_2 nanostructures [28]. In the terahertz frequency region, dielectric constant of VO_2 changes several orders of magnitude when it experiences phase transition. Here we propose a composite VO_2 metasurface with the sandwich microstructure to dynamically regulate absorption properties.

2. Methods

As shown in Fig. 1, the basic unit cell of the designed absorber consists of one air cross hole in VO_2 and a background gold plane with thickness of 0.2 μm which is much larger than the skin depth 0.06 μm to prevent any transmission. The VO_2 patches are separated by a SiO_2 dielectric spacer from the background gold plane. After some carefully calculations based on cruise algorithm, the optimal geometrical parameters are obtained. The chosen width, length, and period of air crosses in simulation are $w = 80$ μm, $l = 172$ μm, and $p = 175$ μm. The thicknesses of VO_2 and SiO_2 are 0.08 μm and 52 μm. A variable conductivity of VO_2 is assumed to mimic phase transition effect. The optical permittivity of VO_2 is described by Drude model $\varepsilon(\omega) = \varepsilon_\infty - \frac{\omega_p^2(\sigma)}{\omega^2 + i\gamma\omega}$ in the terahertz range,

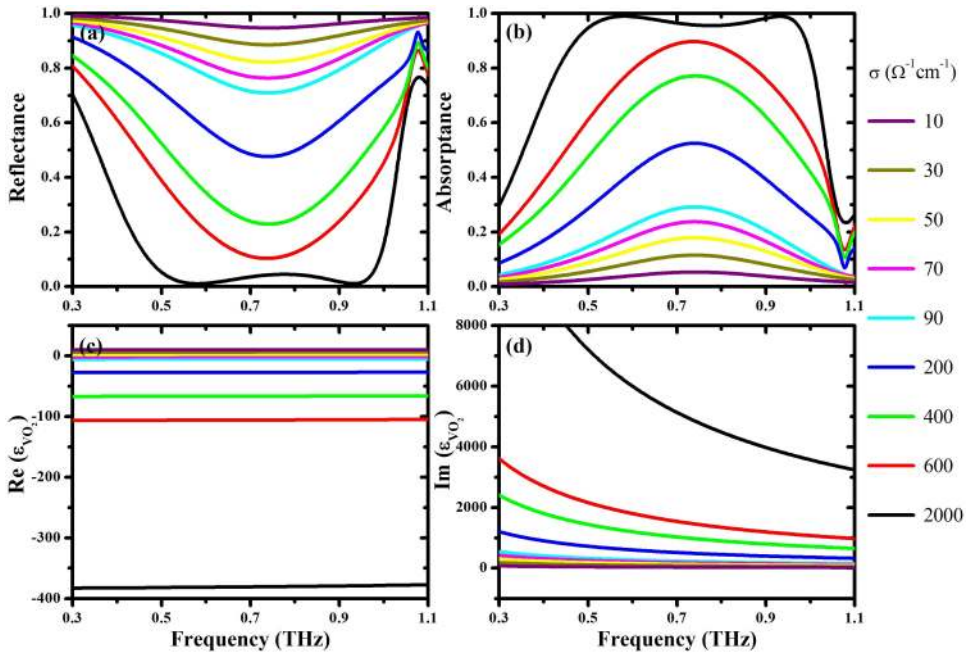

Fig. 2. Calculated reflectance (a) and absorptance (b) spectra with different conductivities of VO_2 under normal incidence. Real (c) and imaginary (d) parts of VO_2 permittivity.

where $\varepsilon_\infty = 12$ is dielectric permittivity at high frequency, $\omega_p(\sigma)$ is the plasma frequency dependent on conductivity and γ is the collision frequency [30], [31]. Besides, $\omega_p^2(\sigma)$ and σ are proportional to free carrier density. The plasma frequency at σ can be approximately described by $\omega_p^2(\sigma) = \frac{\sigma}{\sigma_0}\omega_p^2(\sigma_0)$ with $\sigma_0 = 3 \times 10^3\ \Omega^{-1}\text{cm}^{-1}$, $\omega_p(\sigma_0) = 1.4 \times 10^{15}$ rad/s, and $\gamma = 5.75 \times 10^{13}$ rad/s which is independent of σ. The permittivity of gold is also described by Drude model $\varepsilon_{Au} = 1 - \omega_p^2/\omega(\omega + i\Gamma)$ with plasma frequency $\omega_p = 1.37 \times 10^{16}$ rad/s and collision frequency $\Gamma = 1.2 \times 10^{14}$ rad/s [32]. The dielectric constant of SiO_2 is 3.8 with negligible loss at terahertz frequencies [33], [34].

3. Results

Due to the existence of the bottom 0.2 μm gold film with the skin depth of 0.06 μm to suppress wave transmission (transmittance (T), T = 0), absorptance (A) can be calculated by $A = 1 - R - T = 1 - |S_{11}|^2 - |S_{21}|^2$, where R is the total reflectance. Absorptance can be maximized by minimization of reflectance from the top surface of the proposed structure. To verify our design, full wave electromagnetic simulation (finite element method-Comsol Multiphysics) is performed to get reflectance and then absorptance. Periodic boundary conditions are set in all *xz* and *yz* planes to assume an infinite array. Under normal incidence, simulated absorptance spectra of the proposed absorber are depicted in Fig. 2 with different conductivities. From these simulation results, we can find that when the conductivity of VO_2 is equal to 2000 $\Omega^{-1}\text{cm}^{-1}$, absorptance bandwidth of above 90% absorptance is from 0.47 THz to 0.99 THz, and the central position is at 0.73 THz. But when the conductivity of VO_2 is equal to 10 $\Omega^{-1}\text{cm}^{-1}$, working bandwidth becomes narrow and the biggest value is only 5%. To reveal the tuning mechanism of absorber, real and imaginary parts of VO_2 permittivity as a function of frequency are plotted in Figs. 2(c)–(d). Real and imaginary parts of VO_2 permittivity obviously change in the terahertz range when the conductivity of VO_2 varies from 10 $\Omega^{-1}\text{cm}^{-1}$ to 2000 $\Omega^{-1}\text{cm}^{-1}$. Furthermore, we can see the change of imaginary part under different conductivities is much larger than that of real part. Thus, the central positions of peak keep almost unchanged, but spectral intensity change is very remarkable due to the shift of imaginary part of VO_2 permittivity. So VO_2 can be used for absorption tuning in terahertz spectrum. It can

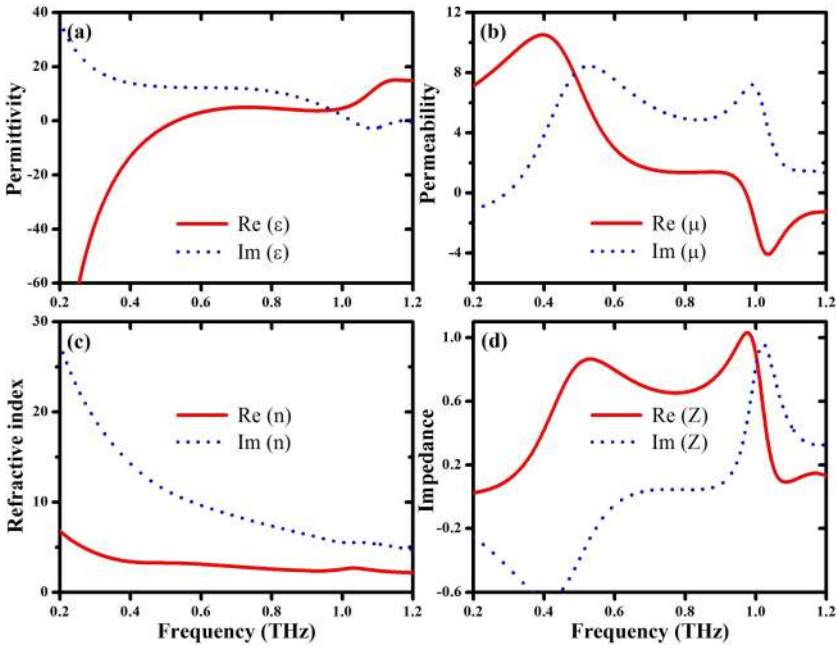

Fig. 3. Retrieved effective physical parameters (a) permittivity, (b) permeability, (c) refractive index, and (d) impedance in the case of perfect absorption when $\sigma = 2000\ \Omega^{-1}\text{cm}^{-1}$.

serve as a tunable material by controlling conductivity, and then working bandwidth and efficiency are dynamically realized.

In order to obtain perfect absorption, impedance of absorber should be matched to that of vacuum. Because the ratio of center wavelength 410.96 μm (0.73 THz) to period 175 μm is $\sim$2.35 under normal incidence, impedance of the designed system can be obtained from the combination of the impedances of air cross hole in VO_2 and a dielectric layer with the ground gold plane. The calculated effective permittivity in Fig. 3(a) is a Drude model, and there is no obvious character. In Fig. 3(b), there are two resonances in permeability, which results in two impedance-matching points. The impedance is normalized to the value 377 Ω of vacuum in Fig. 3(d), and its unit is Ω. The effective impedance of the designed system can be retrieved from $Z = \sqrt{\frac{\mu}{\varepsilon}} = \sqrt{\frac{(1+S_{11})^2 - S_{21}^2}{(1-S_{11})^2 - S_{21}^2}}$, the corresponding real and imaginary parts of the effective impedance are calculated from the inversion of S-parameters method and plotted in Fig. 3(d). Real part of effective impedance of the designed system is almost matched to that of free space, and imaginary part of effective refractive index is very large. As a result, there are two matched bands where reflected wave is minimized.

4. Discussions

Next, the influences of geometrical parameters on absorptance are investigated. We consider the situation where the conductivity of VO_2 is equal to 2000 $\Omega^{-1}\text{cm}^{-1}$, and the thicknesses of VO_2 and SiO_2 are varied. Fig. 4(a) shows calculated absorptance as a function of frequency and thickness of VO_2 with other parameters unchanged under normal incidence. From Fig. 4(a), we can see that absorptance is sensitive to the thickness of VO_2. It results from the fact that imaginary part of VO_2 plays an important role in absorption. When the thickness of VO_2 is very thin, the coupling between VO_2 and metallic substrate is very weak, and the corresponding impedance is not matched to that of vaccum. When the thickness of VO_2 is enough thick, it will strongly reflect electromagnetic wave. Fig. 4(b) shows calculated absorptance as a function of frequency and thickness of SiO_2 with other parameters unchanged under normal incidence. From Fig. 4(b), we can find that when

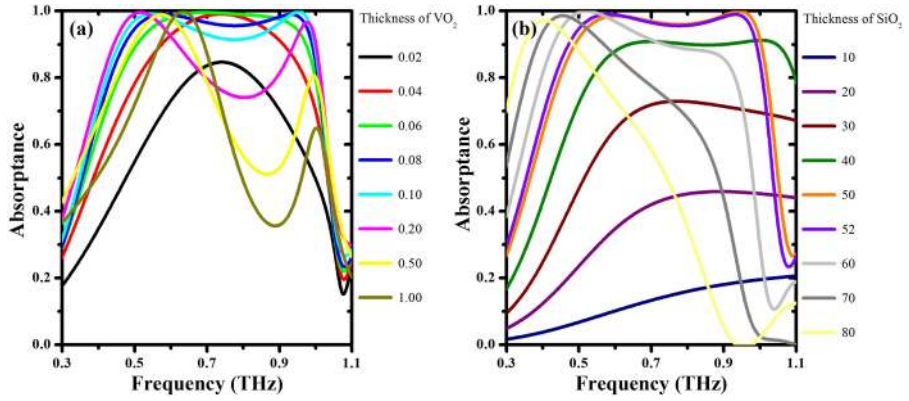

Fig. 4. Calculated absorptance as a function of frequency and thickness of VO_2 (a) and SiO_2 (b) when $\sigma = 2000\ \Omega^{-1}\text{cm}^{-1}$.

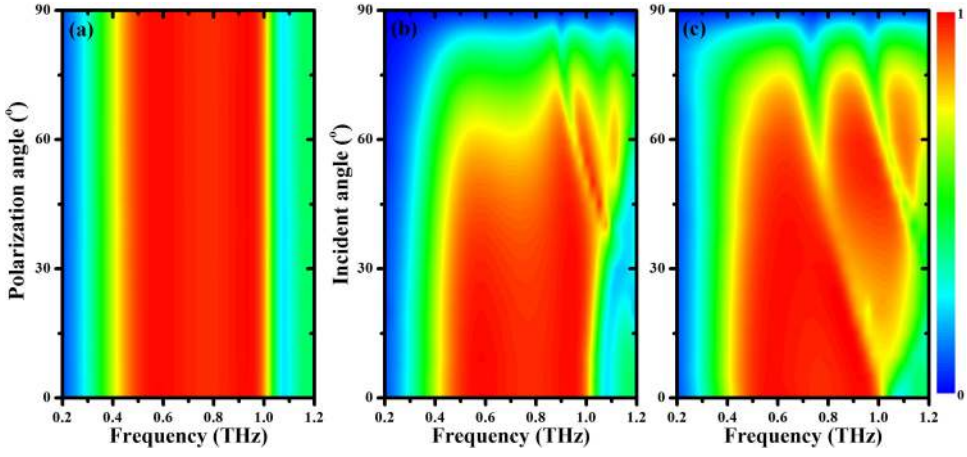

Fig. 5. Calculated absorptance dependence on polarization angle (a) and incidence angle of TE (b) and TM (c) polarizations when $\sigma = 2000\ \Omega^{-1}\text{cm}^{-1}$.

the thickness of SiO_2 is increased, resonance peak will have an obvious red-shift. SiO_2 plays the role of cavity, and different thickness of SiO_2 will have different field distributions, and has different effective impedance. When the thickness of SiO_2 is small, the interaction between metallic structure and VO_2 is very strong. A little change in the thickness of SiO_2 will have an obvious influence on the absorptance spectrum. When the thickness of SiO_2 is enough large, the interaction between metallic structure and VO_2 becomes weak. The thickness of SiO_2 has a great influence on bandwidth and intensity of absorptance and have an optimized value for achieving maximal broadband absorption. It is mainly caused by the fact that impedance-matching condition is strongly dependent on the thickness of SiO_2.

In practical application, polarization insensitivity is an important property for absorber. So it is necessary to consider polarization dependence of the proposed design. Polarization angle is defined between electric field vector and *x* axis in the *xy* plane. Absorptance characteristics under normally incident electromagnetic wave are plotted in Fig. 5(a) with different polarization directions. It can be observed that absorptance spectrum is insensitive to polarization angle, which is attributed to the symmetric property of the designed structure. At the same time, incident angle between wave vector and *z* axis is defined. The influence of incident angle on absorptance characteristics is also investigated. Fig. 5(b) presents absorptance spectra of transverse electric (TE) polarization as a function of frequency and incident angle. It can be seen that absorptance bandwidth remains almost unchanged when incident angle is smaller than 45°. When incident angle continues to increase,

absorptance intensity becomes weaker and then disappears. Fig. 5(c) presents absorptance spectra of transverse magnetic (TM) polarization as a function of frequency and incident angle. When incident angle is larger than 15°, the first absorptance bandwidth becomes narrower and some higher-order modes appear. The ratio of wavelength 300 μm (1.0 THz) to period 175 μm is ~1.71, which is not enough subwavelength for oblique incidence especially at large angle.

5. Conclusion

To summarize, a broadband terahertz absorber has been designed and numerically verified based on a simple VO_2 metasurface. The proposed system shows 71% absorption bandwidth of above 90% absorptance. The proposed absorber has a thin thickness and the ratio of center wavelength 410.96 μm (0.73 THz) to thickness 52.28 μm is ~7.86. Because of periodically simple symmetric patterned structures, absorber is robust against polarization of incident wave. The absorptance average level remains very well for TE-polarized wave with an incident angle up to 45°. The performance of absorption behavior for TM-polarized wave becomes a little worse at incident angle larger than 30° due to higher order scattering. The structure presents the advantages of simple configuration, high absorptance, and broad bandwidth. These properties make it a good candidate for the useful design in photovoltaics, thermal emitter, and stealth technology.

References

[1] J. M. Hao, J. Wang, X. L. Liu, W. J. Padilla, L. Zhou, and M. Qiu, "High performance optical absorber based on a plasmonic metamaterial," *Appl. Phys. Lett.*, vol. 96, no. 25, 2010, Art. no. 251104.

[2] M. Knight, H. Sobhani, P. Nordlander, and N. Halas, "Photodetection with active optical antennas," *Science*, vol. 332, no. 6030, pp. 702–704, 2011.

[3] W. Li and J. Valentine, "Metamaterial perfect absorber based hot electron photodetection," *Nano Lett.*, vol. 14, no. 6, pp. 3510–3514, 2014.

[4] H. A. Atwater and A. Polman, "Plasmonics for improved photovoltaic devices," *Nat. Mater.*, vol. 9, no. 3, pp. 205–213, 2010.

[5] A. Vora, J. Gwamuri, N. Pala, A. Kulkarni, J. M. Pearce, and D. Ö. Güney, "Exchanging Ohmic losses in metamaterial absorbers with useful optical absorption for photovoltaics," *Sci. Rep.*, vol. 4, 2015, Art. no. 4901.

[6] X. Ni, Z. J. Wong, M. Mrejen, Y. Wang, and X. Zhang, "An ultrathin invisibility skin cloak for visible light," *Science*, vol. 349, no. 6254, pp. 1310–1314, 2015.

[7] L. Zhang, S. Zhang, Z. Song, Y. Liu, L. Ye, and Q. H. Liu, "Adaptive decoupling using tunable metamaterials," *IEEE Trans. Microw. Theory Techn.*, vol. 64, no. 9, pp. 2730–2739, Sep. 2016.

[8] H. Xiong, J. S. Hong, C. M. Luo, and L. L. Zhong, "An ultrathin and broadband metamaterial absorber using multi-layer structures," *J. Appl. Phys.*, vol. 114, no. 6, 2013, Art. no. 064109.

[9] T. Jang, H. Youn, Y. J. Shin, and L. J. Guo, "Transparent and flexible polarization-independent microwave broadband absorber," *ACS Photon.*, vol. 1, no. 3, pp. 279–284, 2014.

[10] A. Fardoost, F. G. Vanani, A. Amirhosseini, and R. Safian, "Design of a multilayer graphene-based ultrawideband terahertz absorber," *IEEE Trans. Nano Technol.*, vol. 16, no. 1, pp. 68–74, 2017.

[11] Z. Song, Z. Wang, and M. Wei, "Broadband tunable absorber for terahertz waves based on isotropic silicon metasurfaces," *Mater. Lett.*, vol. 234, pp. 138–141, 2019.

[12] B. Liu, C. Tang, J. Chen, Q. Wang, M. Pei, and H. Tang, "Dual-band light absorption enhancement of monolayer graphene from surface plasmon polaritons and magnetic dipole resonances in metamaterials," *Opt. Exp.*, vol. 25, no. 10, pp. 12061–12068, 2017.

[13] L. Lei, S. Li, H. Huang, K. Tao, and P. Xu, "Ultra-broadband absorber from visible to near-infrared using plasmonic metamaterial," *Opt. Exp.*, vol. 26, no. 5, pp. 5686–5693, 2018.

[14] T. V. Teperik *et al.*, "Omnidirectional absorption in nanostructured metal surfaces," *Nat. Photon.*, vol. 2, no. 5, pp. 299–301, 2008.

[15] H. Xiong, Y. B. Wu, J. Dong, M. C. Tang, Y. N. Jiang, and X. P. Zeng, "Ultra-thin and broadband tunable metamaterial graphene absorber," *Opt. Exp.*, vol. 26, no. 2, pp. 1681–1688, 2018.

[16] W. Guo, Y. Liu, and T. Han, "Ultra-broadband infrared metasurface absorber," *Opt. Exp.*, vol. 24, no. 18, pp. 20586–20592, 2016.

[17] H. Deng, L. Stan, D. A. Czaplewski, J. Gao, and X. Yang, "Broadband infrared absorbers with stacked double chromium ring resonators," *Opt. Exp.*, vol. 25, no. 23, pp. 28295–28304, 2017.

[18] A. Li, Z. Luo, H. Wakatsuchi, S. Kim, and D. F. Sievenpiper, "Nonlinear, active, and tunable metasurfaces for advanced electromagnetics applications," *IEEE Access*, vol. 5, pp. 27439–27452, 2017.

[19] A. Li, S. Singh, and D. Sievenpiper, "Metasurfaces and their applications," *Nanophotonics*, vol. 7, no. 6, pp. 989–1011, 2018.

[20] A. Li, S. Kim, Y. Luo, Y. Li, J. Long, and D. F. Sievenpiper, "High-power transistor-based tunable and switchable metasurface absorber," *IEEE Trans. Microw. Theory Techn.*, vol. 65, no. 8, pp. 2810–2818, Aug. 2017.

[21] P. Yu *et al.*, "Broadband metamaterial absorbers," *Adv. Opt. Mater*, vol. 6, 2018, Art. no. 1800995.
[22] P. Yu *et al.*, "Metamaterial perfect absorber with unabated size-independent absorption," *Opt. Exp.*, vol. 26, no. 16, pp. 20471–20480, 2018.
[23] Y. Huang, G. Wen, W. Zhu, J. Li, L. M. Si, and M. Premaratne, "Experimental demonstration of a magnetically tunable ferrite based metamaterial absorber," *Opt. Exp.*, vol. 22, no. 13, pp. 16408–16417, 2014.
[24] W. Zhu *et al.*, "Wideband visible-light absorption in an ultrathin silicon nanostructure," *Opt. Exp.* vol. 25, no. 5, pp. 5781–5786, 2017.
[25] W. Zhu *et al.*, "MoS_2 broadband coherent perfect absorber for terahertz waves," *IEEE Photon. J.*, vol. 8, no. 6, Dec. 2016, Art. no. 5502207.
[26] W. Huang, X. Yin, C. Huang, Q. Wang, T. Miao, and Y. Zhu, "Optical switching of a metamaterial by temperature controlling," *Appl. Phys. Lett.*, vol. 96, no. 26, 2010, Art. no. 261908.
[27] M. A. Kats *et al.*, "Ultra-thin perfect absorber employing a tunable phase change material," *Appl. Phys. Lett.*, vol. 101, no. 22, 2012, Art. no. 221101.
[28] H. Kocer *et al.*, "Thermal tuning of infrared resonant absorbers based on hybrid gold-VO_2 nanostructures", *Appl. Phys. Lett.*, vol. 106, no. 16, 2015, Art. no. 161104.
[29] M. Liu *et al.*, "Terahertz-field-induced insulator-to-metal transition in vanadium dioxide metamaterial," *Nature*, vol. 487, no. 7407, pp. 345–348, 2012.
[30] S. Wang, L. Kang, and D. H. Werner, "Hybrid resonators and highly tunable terahertz metamaterials enabled by vanadium dioxide (VO_2)," *Sci. Rep.*, vol. 7, pp. 4326, 2017.
[31] Q. Chu, Z. Song, and Q. H. Liu, "Omnidirectional tunable terahertz analog of electromagnetically induced transparency realized by isotropic vanadium dioxide metasurfaces," *Appl. Phys. Exp.*, vol. 11, no. 8, 2018, Art. no. 082203.
[32] N. Liu *et al.*, "Plasmonic analogue of electromagnetically induced transparency at the Drude damping limit," *Nat. Mater.*, vol. 8, no. 9, pp. 758–762, 2009.
[33] M. Naftaly and R. E. Miles, "Terahertz time-domain spectroscopy of silicate glasses and the relationship to material properties," *J. Appl. Phys.*, vol. 102, no. 4, 2007, Art. no. 043517.
[34] R. Malureanu *et al.*, "A new method for obtaining transparent electrodes," *Opt. Exp.*, vol. 20, no. 20, pp. 22770–22782, 2012.